*National Conference in Mechanical Engineering Research and Postgraduate Studies (2nd NCMER 2010)*
*3-4 December 2010, Faculty of Mechanical Engineering, UMP Pekan, Kuantan, Pahang, Malaysia; pp. 100-116*
*ISBN: 978-967-0120-04-1; Editors: M.M. Rahman, M.Y. Taib, A.R. Ismail, A.R. Yusoff, and M.A.M. Romlay*


# PREDICTION OF FATIGUE LIFE ON LOWER SUSPENSION ARM SUBJECTED TO VARIABLE AMPLITUDE LOADING

**Z. Husin, M.M. Rahman, K. Kadirgama, M.M. Noor and Rosli A. Bakar**

Faculty of Mechanical Engineering, Universiti Malaysia Pahang
Tun Abdul Razak Highway, 26600 Pekan, Kuantan, Pahang, Malaysia
Email: mustafizur@ump.edu.my

## ABSTRACT

This paper focuses on the finite element based fatigue life prediction of lower suspension arm, subjected to variable amplitude loading. The objectives of this study are to predict fatigue life of the lower suspension arm using stress-life and strain-life methods, to investigate the effect of the mean stress. The lower suspension arm was developed using computer aided design software. The finite element modeling and analysis were performed utilizing the finite element analysis code. Mesh was created using tetrahedral 10 nodes element. The finite element analysis then was performed using MSC.NATRAN code using the linear elastic approach. In addition, the fatigue life was predicted using the stress-life and strain-life approach subjected to variable amplitude loading. The three types of variable amplitude are considered in this study. The TET10 and maximum principal stress were considered in the linear static stress analysis and the critical location. From the fatigue analysis, Goodman method is conservative method when subjected to SAETRN and SAESUS loading histories while SWT method is more conservative in SAEBKT loading histories. Stress-life method is capable to give higher fatigue life when subjected to bracket mean loading (SAEBKT) while strain-life method is capable to give higher fatigue life when subjected to positive mean loading (SAETRN) and negative mean loading (SAESUS). From the material optimization, 7175-T73 aluminum alloy is suitable material of the suspension arm.

***Keywords:*** Lower Suspension arm, aluminum alloy, FEM, variable amplitude loading, stress-life, strain-life,

## INTRODUCTION

Suspension is the system of linkages and springs or shocks that allows the wheels to move up and down independent of the body. This is important for absorbing bumps in rough terrain, gracefully landing jumps, and getting the right amount of body lean and weight transfer in turns. Both end of this component are fixed to the wheel and the chassis. Suspension components, along with wheel rims and brake components are un-sprung masses, which make weight reduction important for ride quality and response as well as for reducing the total vehicle weight. Every automotive suspension has two goals, passenger comfort and vehicle control. Comfort is provided by isolating the vehicle's passengers from road disturbances like bumps or potholes. Control is achieved by keeping the car body from rolling and pitching excessively, and maintaining good contact between the tire and the road. This fatigue analysis needs the method that related to the analysis about the stress, strain, and fracture mechanics of background study, by using the variable amplitude loading. These are important subject the safety of the lower suspension arm can be analyzed due to the result obtained from the finite element analysis. The safety aspect of the component is the important factor to develop the automotive industry. The most of the failure observed in the real structure and mechanical component are due to the fatigue. In the design of the real system subjected to the environment loadings, both the fatigue strength and dynamic properties of the external loads are important. In automotive industry, aluminium (Al) alloy has limited usage due to their higher cost and less developed manufacturing process compared to steels. However, Al alloy has the advantage of lower weight and therefore has been used increasingly in car industry for the last 30 years, mainly as engine block, engine parts, brake components, steering components and suspension arms where significant weight can be achieved. The increasing use of Al is due to the safety, environmental and performance benefits that aluminum offers, as well as the improved fuel consumption because of light weight. In this project, the material used for the suspension arm is a AA5083 alumnium alloy, which has good formability and corrosion resistance as well as high impact and fatigue strength. One of the important structural limitations of an aluminium alloy is its fatigue properties. This study is aimed at the automotive industry, more specifically a wrought aluminium suspension system, where safety is of great concern. Most of the time to failure consists of crack initiation and a conservative approach is to denote the component as failed when a crack has initiated Kyrre et al. (2005). This simplification allows designers to use linear elastic stress results obtained from multibody dynamic FE (finite element) simulations for fatigue life analysis. The lower suspension arm is facing the vibration from the variation of road surface. Therefore it is subjected to cyclic loading and it is consequently prone to fatigue damage. The stress from the wheel unit and the shock absorber that are acting on the lower suspension arm can be analyzed from this finite element analysis. The best design of the lower suspension arm is considered for benefit of the cost management of the production. The best material that will be used for the manufacturing process of the component is important to predict the life or fracture expectation.

Rahman et al. (2007) were studied about finite element based durability assessment in a two- stroke free piston linear engine component using variable amplitude loading. Authors discussed the finite element analysis to predict the fatigue life and identify the critical locations of the component. The effect of mean stress on the fatigue life also investigated. The linear static finite element analysis was performed using MSC. NASTRAN. The result was capable of showing the contour plots of the fatigue life histogram and damage histogram at the most critical location. Rahman et al. (2009) were conducted fatigue life prediction of lower suspension arm using strain-life approach. From the fatigue analysis, Smith-Watson-Topper mean stress correction was conservative method when subjected to SAETRN loading, while Coffin-Manson model is applicable when subjected to SAESUS and SAEBRKT loading. From the material optimization, 7075-T6 aluminum alloy is suitable material of the suspension arm. Conle and Mousseau (1991) used the vehicle simulation and finite element result to generate the fatigue life contours for the chassis component using automotive proving ground load history result combine with the computational techniques. They concluded that the combination of the dynamics modeling, finite element analysis is the practical techniques for the fatigue design of the automotive component.

Kyrre et al. (2005) were conducted the fatigue life prediction of suspension arm using finite element analysis of surface topography. They concluded that fatigue strength of the structure is highly depending on the surface quality. Current methods to predict fatigue life rely on empirical relations between geometric surface parameters and observed endurance lives. The uncertainty associated with these methods is typically high, since parameters based on geometrical averages can fail to describe important characteristics of surface topography. Then they proposed a new approach where detailed finite element analysis of surface topography is used as a foundation for fatigue life prediction. Kim et al. (2002) studied a method for simulating vehicles dynamic loads, but they add durability assessment. For their multibody dynamic analysis they use DADS and a flexible body model. The model was for a transit bus. For their dynamic stress analysis, MSC. NASTRAN was used. The fatigue life was then calculated using a local strain approach. From the fatigue life, it was found that the majority of the fatigue damage occurred over a frequency range that depend on terrain traveled (service or accelerated test course). This showed that the actual service environment could be simulated instead of using an accelerated testing environment. Nadot and Denier ( 2003) have been studied fatigue phenomena for nodular cast iron automotive suspension arms. They found that the major parameter influencing fatigue failure of casting components are casting defects. The high cycle fatigue behaviour is controlled mainly by surface defects such as dross defects and oxides while the low cycle fatigue is governed by multiple cracks initiated independently from casting defects.

Svensson et al. (2005) was conducted the fatigue life prediction based on variable amplitude tests-specific applications. Three engineering components have been tested with both constant amplitude loading and different load spectra and the results are analysed by means of a new evaluation method. The method relies on the Palmgren-Miner hypothesis, but offers the opportunity to approve the hypothesis validity by narrowing the domain of its application in accordance with a specific situation. In the first case automotive spot weld components are tested with two different synthetic spectra and the result is extrapolated to new service spectra. In the second case, the fatigue properties of a rock drill component are analyzed both by constant amplitude tests and by spectrum tests and the two reference test sets are compared. In the third case, butt welded mild steel is analyzed with respect to different load level crossing properties and different irregularity factors. Molent et al. (2007) was evaluated the spectrum fatigue crack growth using variable amplitude data. This paper summarizes a recent semi-empirical model that appears to be capable of producing more accurate fatigue life predictions using flight load spectra based on realistic in-service usage. The new model described here provides an alternative means for the interpretation of full-scale and coupon fatigue test data, and can also be used to make reliable life predictions for a range of situations. This is a very important capability, particularly where only a single full-scale fatigue test can be afforded and should lead to more economical utilization of airframes. Nolting et al. ( 2008) was investigated the effect of variable amplitude loading on the fatigue life and failure mode of adhesively bonded double strap (DS) joints made from clad and bare 2024-T3 aluminum. They concluded that the fatigue life of a variable amplitude loading spectra can be calculated with reasonable accuracy using an effective stress range vs. life fatigue curve. The effective stress range vs. failure life curve is dependent on the bond geometry and therefore this curve must be developed for each component geometry of interest. The effective stress range versus life fatigue curve should be used to predict the fatigue life of clad specimens if the failure mode of the clad specimens is expected to be adhesive failure.

## FINITE ELEMENT BASED FATIGUE LIFE ANALYSIS

Fatigue analysis has traditionally been performed at a later stage of the design cycle. This is due to the fact that the loading information could only be derived from the direct measurement, which requires a prototype (Bannantine et al., 1990; Stephens et al, 2001). Multibody dynamics (MBD) (Kim et al., 2002) is capable of predicting the component loads which enable designer to undertake a fatigue assessment even before the prototype is fabricated. The purpose of analyzing a structure early in the design cycle is to reduce the development time and cost. This is achieved by determining the critical region of the structure and improving the design before prototype are built and tested. The finite element (FE) based on fatigue analysis can be considered as a complete engineering analysis for the component. The fatigue life can be estimated for every element in the finite element model, and the contour plots of life damage can be obtained. The geometry information is provided by the FE result for each load case applied independently. Appropriate material properties are also provided for the desired fatigue analysis method. An integrated approach to fatigue life analysis combines the multibody dynamic analysis, finite element analysis, and the fatigue analysis into a consistent entity for the prediction of the fatigue life of a component Rahman et al. (2007). The flowchart of the finite element based fatigue analysis is shown in Figure 1.

**Stress-Life Method**

The stress life *(S-N)* method was first applied over hundred years ago (Wöhler, 1867) and consider nominal elastic stresses and how they related to life. This approach to the fatigue analysis of components works well for situations in which only elastic stresses and strains are present. However, most components may appear to have nominally cyclic elastic stresses but stress concentration are present in the component may result in load cyclic plastic deformation (Rahman et al., 2007b). The *S-N* approach is still widely used in design applications where the applied stress is primary within the elastic range of the material and the resultant lives (cycles to failure) are long, such as power transmission shaft. The stress-life method does not work well in low-cycle applications, where the applied strain have significant plastic component. The dividing line between low and high cycle fatigue depends on the material being considered, but usually falls between 10 and $10^5$ cycles [Banantine et al., 1990].

The stress-life approach was the first well-developed approach to the fatigue analysis. It is suitable to predict high cycle fatigue and has been extensively used in automotive industry. Fatigue life depends primarily on loads, materials, geometry and environmental effects and it's usually described by *S-N* curve. The stress-based approach considers the controlling parameters for fatigue life to nominal stress. The relationship between the nominal stress amplitude and fatigue life is often represented as *S-N* curve, which can expressed in Eq. (1)

$$\sigma_a = \sigma'_f (2N_f)^b \tag{1}$$

where $\sigma_a$ is stress amplitude, $\sigma'_f$ is a fatigue coefficient, $2N_f$ is the reveals to failure and $b$ is the fatigue strength exponent (Rahman et al., 2007b). The modified Goodman and Gerber equations are given by Equations (2) and (3) respectively. The *S-N* curves shows in Figure 2.

$$\frac{\sigma_a}{S_e} + \frac{\sigma_m}{S_u} = 1 \tag{2}$$

$$\frac{\sigma_a}{S_e} + \left(\frac{\sigma_m}{S_u}\right)^2 = 1$$
(3)

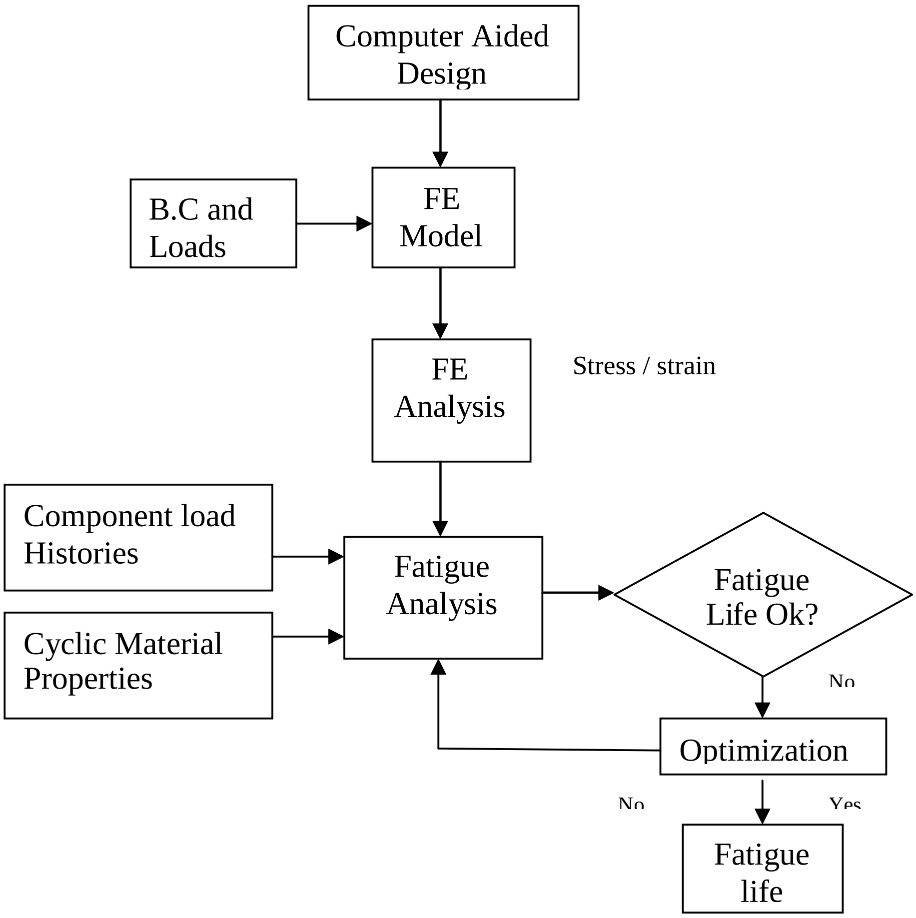


Figure 1: The finite element based fatigue analysis

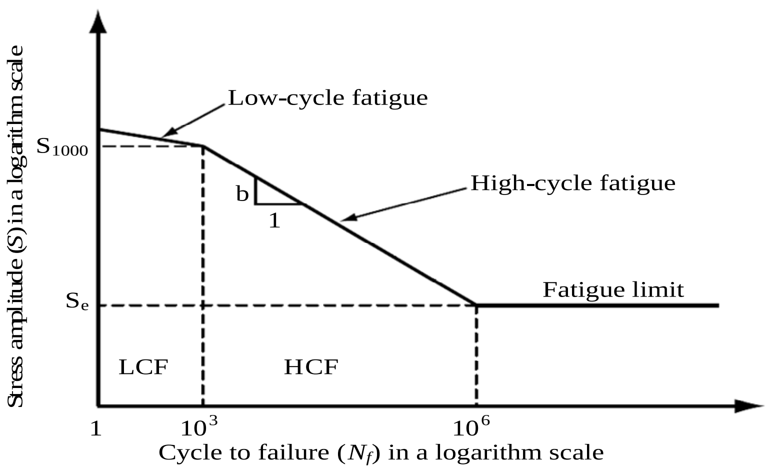


Figure 2: *S-N* curve

## Strain-Life Method

The strain-life method is based on the observation that in many components the response of the material in critical location (notches) is strain or deformation dependent. When loads are low, stress and strain are linearly related. Consequently, in this range, load-controlled and strain-controlled test results are equivalent. The stress –life data are generated from load-controlled test. At high load levels, in the low cycle fatigue (LFC) regime, the cyclic stress-strain response and the material behaviour are best model under strain-controlled conditions. The local strain-life approach is preferred if the loading history is irregular and where the mean stress and the loads sequence effect are thought to be important. The operations involved in the prediction process must be performed sequentially. First, the stress and the strain region are estimated and then the rainflow cycle counting method Matsuishi and Endo (1968) is used to the load-time history into a strain-time history. The next step is to use the finite element method to convert the reduced load-time history and also to calculate the stress and strain in the highly stressed area. Then, the crack initiations method is employed to predict the fatigue life. The simple linear hypothesis proposed by Palmgren (1924) and Miner (1945) is used to accumulate the fatigue damage. Finally, the damage values for all cycles are summed until a critical damage sum (failure criteria) is reached. A typical strain-life curves based on Coffin-Manson relationship are shown in Figure 3. The Coffin-Manson total strain-life is mathematically defined as

$$\frac{\Delta\varepsilon}{2} = \frac{\sigma'_f}{E}(2N_f)^b + \varepsilon'_f(2N_f)^c \tag{4}$$

Morrow elastic term in the strain-life equation by mean stress, $\sigma_m$.

$$\varepsilon_a = \frac{\sigma'_f - \sigma_m}{E}(2N_f)^b + \varepsilon'_f(2N_f)^c \tag{5}$$

Smith-Watson-Topper (SWT) mean stress correction is mathematically defined as

$$.\ \sigma_{\max}\varepsilon_a E = (\sigma'_f)^2(2N_f)^{2b} + \varepsilon'_f\varepsilon' E(2N_f)^{b+c} \tag{6}$$

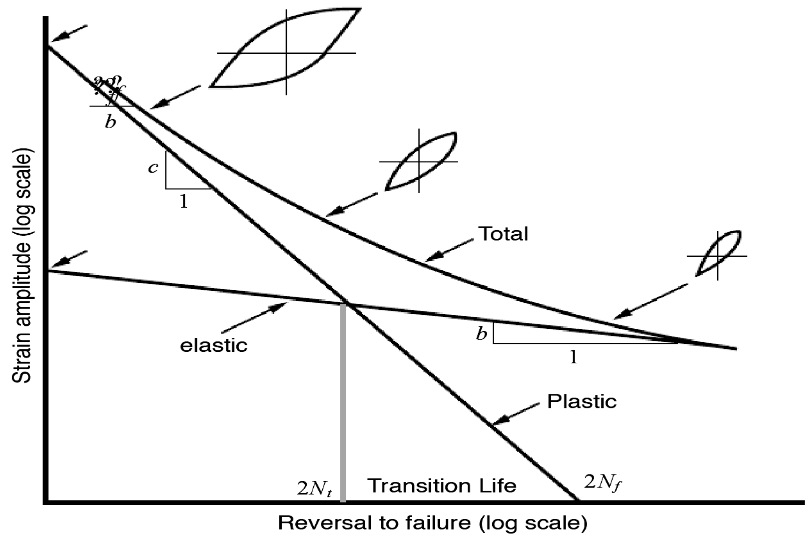


Figure 3: The typical strain-life curve

## Material Information

Material model and material properties play an important role in the result of the FE method. The material properties are one of the major inputs which is the definition of how a material behaves under the cyclic loading conditions. The cyclic material properties are used to calculate the elastic-plastic stress-strain response and the rate at which fatigue damage accumulate due to each fatigue cycle. The materials parameters required depend on the analysis methodology being used. The mechanical properties of 5083-87 Aluminium alloy are shown in Table 1.

Table 1: Mechanical properties of aluminum alloy 5083-87

| **Monotonic Properties** | **Value** | **Unit** | **Cyclic properties** | **Value** | **Unit** |
|---|---|---|---|---|---|
| Tensile strength, $\sigma_{UTS}$ | 385 | MPa | Fatigue strength exponent, $b$ | -0.094 | |
| Yield strength, $\sigma_{YS}$ | 285 | MPa | Fatigue strength coefficient, $\sigma'_f$ | 650 | MPa |
| Young's modulus, $E$ | 69 | GPa | Fatigue ductility exponent, $c$ | -1.01 | |
| Strain hardening exponent, $n$ | 0.081 | | Fatigue ductility coefficient, $\varepsilon'_f$ | 2.26 | |

## Loading Information

Loading is another major input to the finite element based fatigue analysis. Several types of variable amplitude loading history were selected from the Society of Automotive Engineers (SAE) profiles. The component was loaded with three time histories, corresponding to typical histories for transmission, suspension and bracket components at different load levels. The first load history has a predominantly tensile (positive) mean which reflects sudden changes in mean, which is referred to as the transmission history. The second load history has a predominantly compressive (negative) mean, which is referred as suspension history. The third load history representing a vibration with nearly zero mean loads, which is referred as the bracket history (Tucker and Bussa, 1975; Rahman *et al*., 2007). These histories were scaled to two peak strain levels and used as full-length histories. The variable amplitude load-time histories are shown in Figure 4.

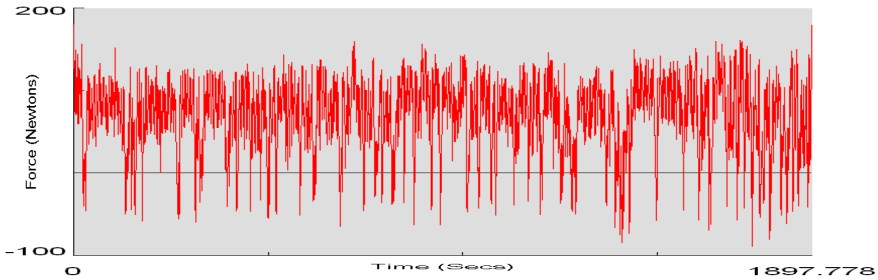

(a) SAETRN loading-time histories

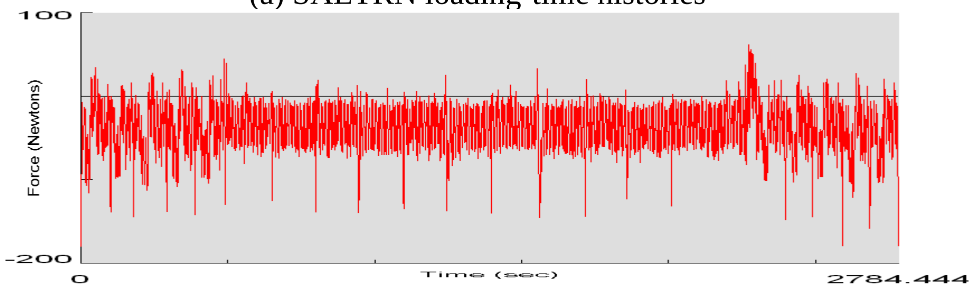

(b) SAESUS loading-time histories

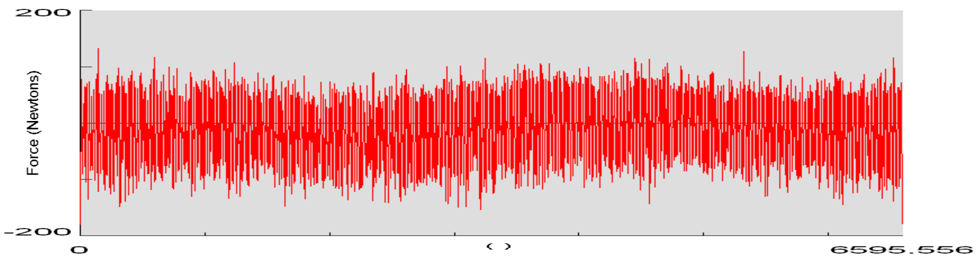

(c) SAEBRKT loading-time histories

Figure 4: The variable amplitude load-time histories

## RESULTS AND DISCUSSION

### Finite Element Modeling

The lower suspension arm is facing the vibration from the variation of road surface. Therefore it is subjected to cyclic loading and it is consequently prone to fatigue damage. The stress from the wheel unit and the shock absorber that are acting on the lower suspension arm can be analyzed from this finite element analysis. Three-dimensional model geometry was developed in SOLIDWORK software. The structural model and overall dimensions of suspension arm as shown in Figure 5. A 10 nodes tetrahedral element was used for the solid mesh. A sensitivity analysis was performed to obtain the optimum element size. These analysis were performed iteratively a different element lengths until the solution obtain appropriate accuracy. Convergence of the stresses was observed, as the mesh size was successively refined. The mesh global length of 0.3 mm was considered and the force 180 N was applied one end of the bushing that connected to the tyre. The other two bushing that connected to the body of the car are constraint. The three-dimensional FE model, loading and constraints of suspension arm is shown in Figure 6.

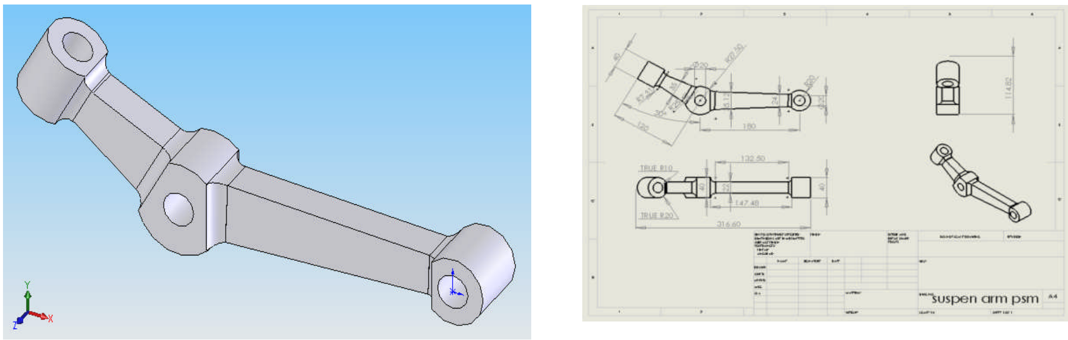

Figure 5: Structural model and overall dimensions of suspension arm

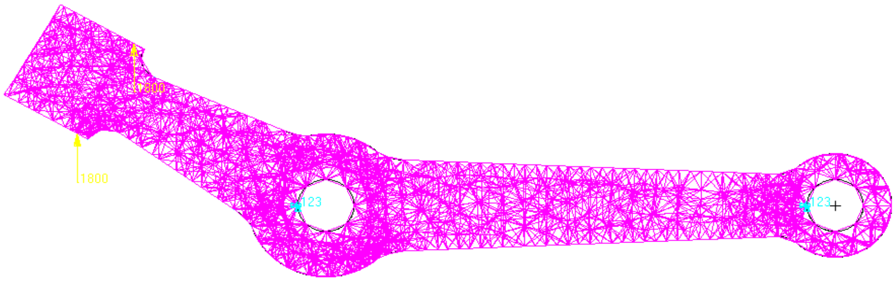


Figure 6: Three-dimensional FE model, loading and constraints

**Selection of Mesh Type**

Mesh study is performed on the FE model to ensure sufficiently fines sizes are employed for accuracy of calculated results but at competitive cost (CPU time). In the process, specified field variable is selected and its convergence is monitored and evaluated. Selecting the right techniques of meshing are based on the geometry, model topology, analysis objectives. Tetrahedral meshing produces high quality meshing for boundary representation solids model imported from the most CAD system. The finite element model using TET10 and TET4 type of elements as shown in Figure 7 and von Mises stress contour is shown in Figure 8 for TET10 and TET4 elements. Analysis shown that TET10 mesh predicted higher von Mises stress than the TET4 mesh (Figure 7) various mesh global length. Then, the comparison was made between these two elements based on von Mises, Tresca, maximum principal stresses and displacement are tabulated in Table 2 and 3 for TET 10 and TET4 respectively. According to the results from Table 2 and 3, it can be seen that the TET10 are able to capture the higher stresses compared to TET4 for the same mesh global length. Thus, TET10 is used for overall analysis. Variation of maximum principal stresses and displacement against the global mesh length are shown in Figure 9 and 10 respectively. It can be seen that the TET10 gives the higher stress and displacement throughout the global mesh length.

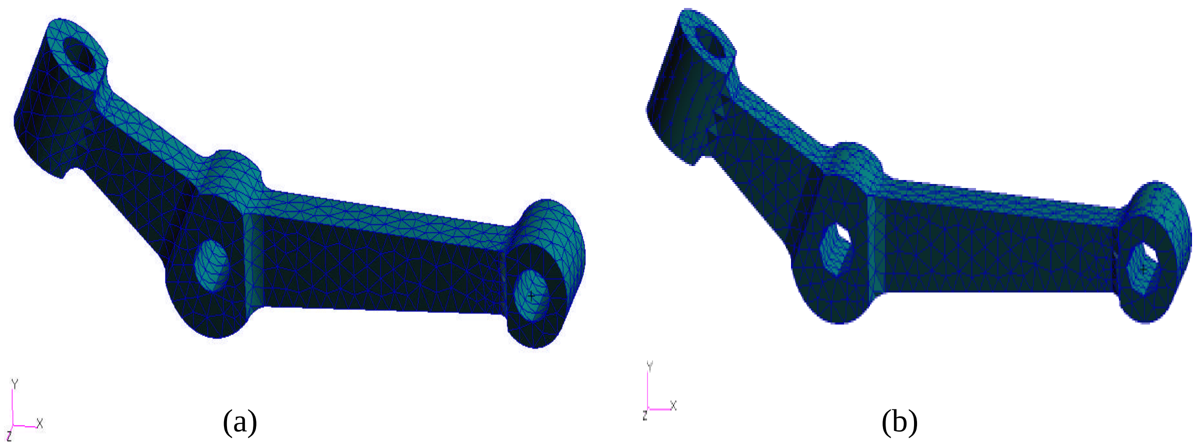

(a) (b)

Figure 7**:** (a) TET10, 5834 elements and 9844 nodes; (b) TET4, 5831 elements and 1511 nodes

Table 2: Variation of stresses at critical location for TET10 mesh.

| **Mesh Size (mm)** | **Number of Node** | **Number of Element** | **von Mises (MPa)** | **Tresca (MPa)** | **max principal stress (MPa)** | **Displacement (mm)** |
|---|---|---|---|---|---|---|
| 0.3 | 1467 | 5634 | 77 | 79 | 81 | 0.016 |
| 0.4 | 1204 | 4404 | 70 | 71 | 71 | 0.013 |
| 0.6 | 1044 | 3827 | 53 | 57 | 60 | 0.011 |
| 1.2 | 820 | 3019 | 45 | 46 | 47 | 0.010 |
| 1.6 | 622 | 2132 | 44 | 45 | 46 | 0.009 |
| 2.0 | 396 | 1248 | 34 | 36 | 37 | 0.007 |

Table 3: Variation of stresses at critical location for TET4 mesh.

| **Mesh Size (mm)** | **Number of Node** | **Number of Element** | **von Mises (MPa)** | **Tresca (MPa)** | **max principal stress (MPa)** | **Displacement (mm)** |
|---|---|---|---|---|---|---|
| 0.3 | 1467 | 5634 | 77 | 79 | 81 | 0.016 |
| 0.4 | 1204 | 4404 | 70 | 71 | 71 | 0.013 |
| 0.6 | 1044 | 3827 | 53 | 57 | 60 | 0.011 |
| 1.2 | 820 | 3019 | 45 | 46 | 47 | 0.010 |
| 1.6 | 622 | 2132 | 44 | 45 | 46 | 0.009 |
| 2.0 | 396 | 1248 | 34 | 36 | 37 | 0.007 |

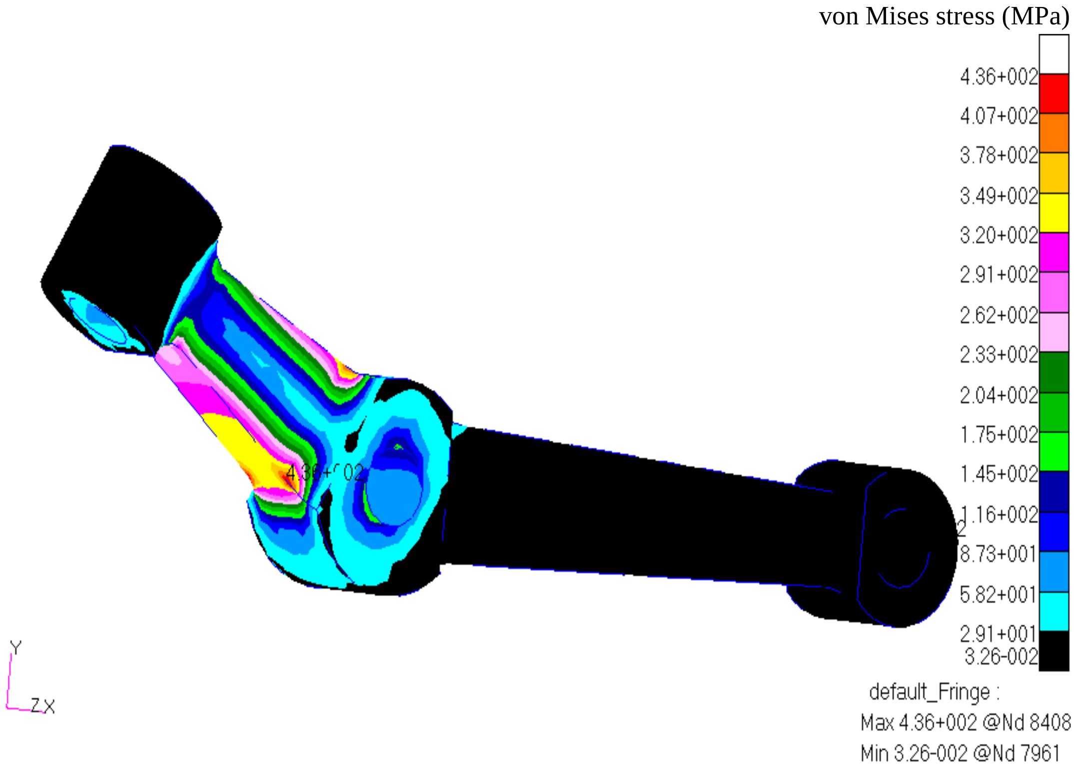


(a) for TET 10

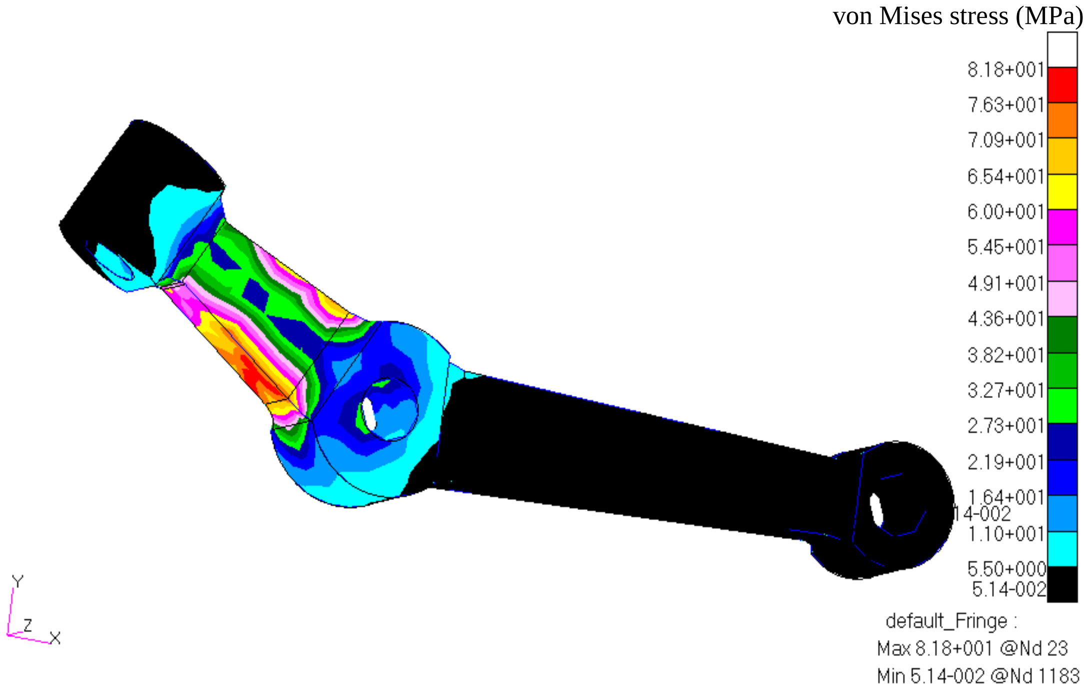


(b) for TET 4

Figure 8: von Mises stresses contours (a) for TET 10; (b) for TET 4

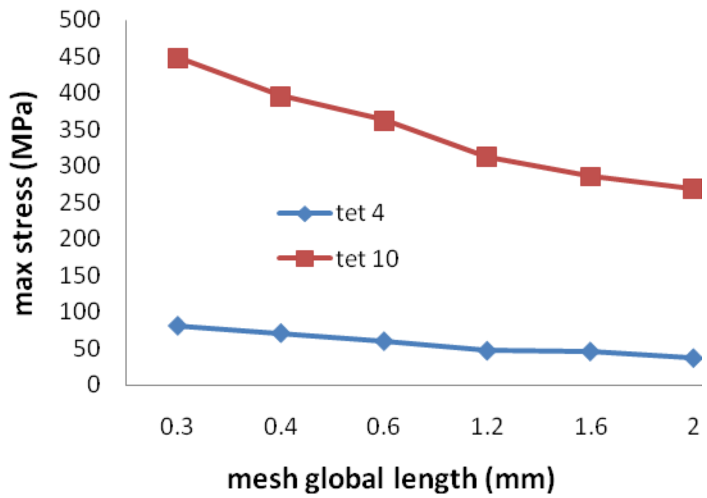


Figure 9: Variation of maximum principal stresses for different element types

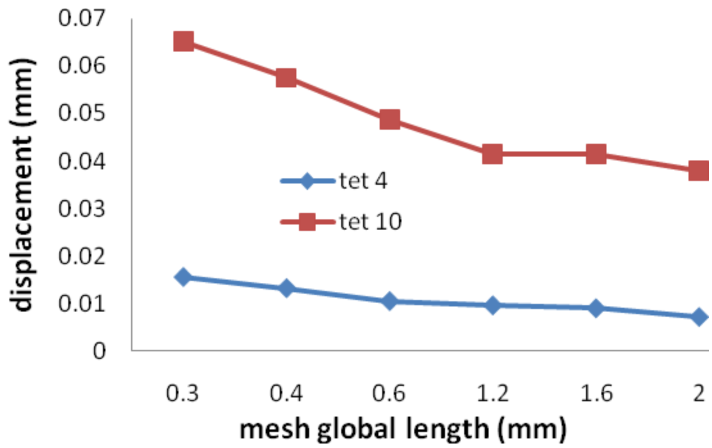


Figure 10: Variation of maximum displacement for different element type

**Identification of Mesh Convergence**

The convergence of the stress was considered as the main criteria to select the mesh size. The finite element mesh was generated using the TET10 for various mesh global length. Figure 11 shows the predicted results of stresses at the critical location of the suspension arm. It can be seen that the smaller the mesh size capture the higher predicted stresses. It is concluded from the figure that the maximum principal stresses is suitable for fatigue analysis. It can seen that mesh size of 0.3 mm (5585 elements) has obtained the maximum stresses. The smaller mesh size than 0.3mm is not implemented due the limitation of computational time (CPU time) and storage capacity of the computer. Therefore, the maximum principal stress based on TET10 at 0.3 mm mesh size is used in the fatigue life analysis cause of the stress is higher compared to Von Mises and Tresca principal stress.

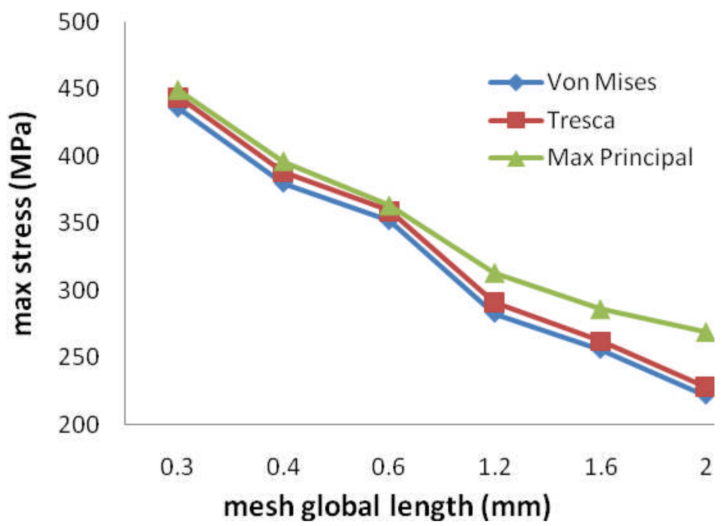


Figure 11: Stresses versus mesh size at critical location for TET10 to check mesh convergence

**Linear Elastic Stress Analysis**

The linear static analysis was performed using MSC. NASTRAN software to determine the stress and strain results from the finite element model. The material utilized in this work consists of a linear elastic, isotropic material. The choice of the linear elastic material model is essentially mandated. Model loading consist of the applied mechanical load, which is modeled as the load control and the displacement control. From the analysis, the fillet of the bushing is found to experience the largest stresses. Hence, the result of the maximum principal stresses is used for the fatigue life analysis. The maximum principal stresses distributions of the suspension arm for the linear static stress analysis is shown in Figure 12 for 5083-87 Aluminum alloy. From the result, the maximum principal stresses of 449 MPa occurred at node 7092.

**Fatigue Analysis**

The fatigue life of the suspension arm is initially predicted using 5083-87 aluminum alloy with SAETRN loading using the stress-life and strain-life method. This analysis is focused on the critical location at node of 8408. The fatigue life is expressed in second for the variable amplitude loading. It is observed that the fillet of middle bushing that connected to absorber is the most critical location of the suspension arm. This analysis is done to determine the fatigue life using the stress-life and strain-life method based on various variable amplitude loading time histories such as SAERTN (positive mean loading), SAESUS (negative mean loading) and SAEBRKT (bracket mean loading) as shown in Table 4 and Table 5 respectively. From Table 4 and Table 5, the fatigue life of the suspension at the critical location of node (8408) for various loading histories is different. The SAESUS loading histories gives the higher life compared to SAETRN and SAEBKT loading histories. Goodman method is more conservative method compared to Gerber and no mean stress correction method for prediction using the stress-life method while for the prediction using strain-life method, Smith-Watson Topper (SWT) mean stress correction method is more conservative method compared to

Coffin-Manson and Morrow method. The distribution of fatigue life in term of log of life (sec) contour plotted for 5083-87 aluminum alloy using stress-life and strain-life method with SAETRN (positive mean loading) are showed in Figure 13 and Figure 14 respectively.

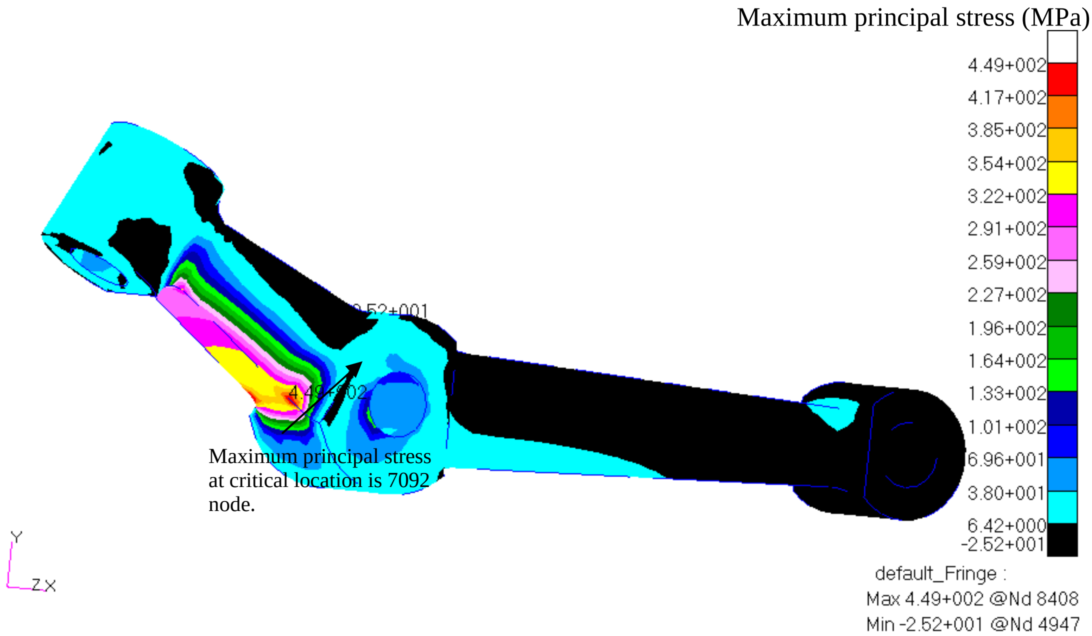


Figure 12: Maximum principal stresses contour plotted for 5083-87 aluminum alloy with SAETRN loading

Table 4: Fatigue life at critical location of node (8408) for various loading histories for 5083-87 by using stress-life method.

| Mean Stress Correction Method | Fatigue life (cycles) | | |
|---|---|---|---|
| | SAETRN | SAESUS | SAEBKT |
| No correction | 2290 | 11481 | 389 |
| Goodman | 251 | 588 | 195 |
| Gerber | 1288 | 10715 | 426 |

Table 5: Fatigue life at critical location of node (8408) for various loading histories for 5083-87 by using strain-life methods

| Mean Stress Correction Method | Fatigue life (cycles) | | |
|---|---|---|---|
| | SAETRN | SAESUS | SAEBKT |
| Coffin-Manson | 759 | 3388 | 126 |
| Morrow | 447 | 2238 | 129 |
| SWT | 323 | 1514 | 120 |

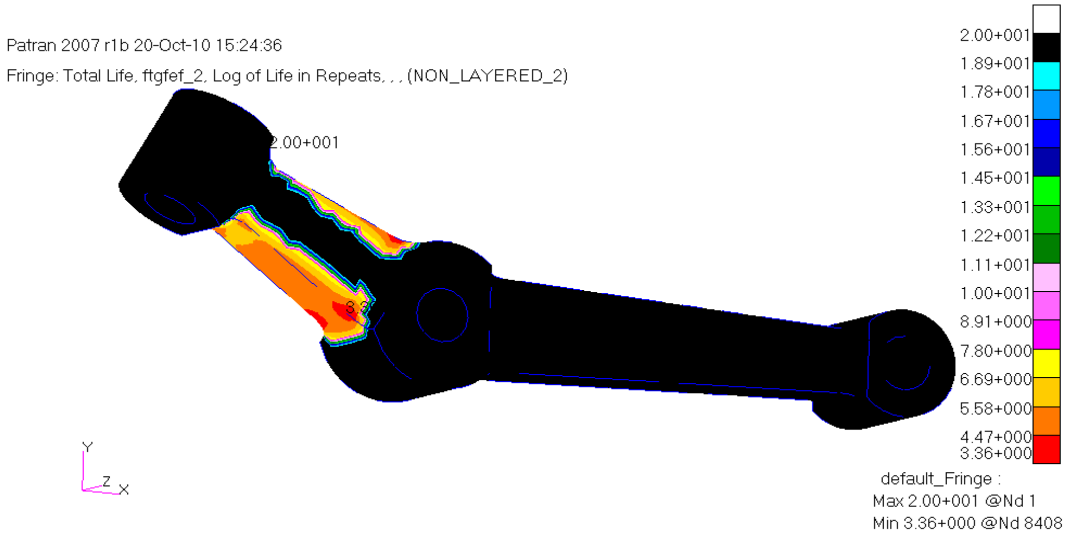


Figure 13: Predicted life contours plotted in term of log of life for 5083-87 aluminum alloy with SAETRN loading by using stress-life method.

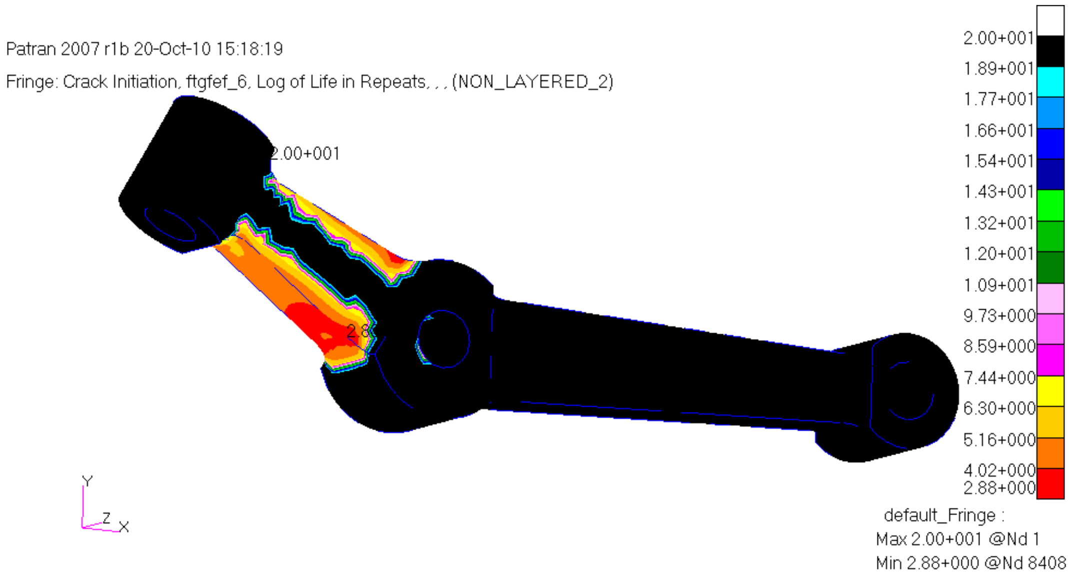


Figure 14: Predicted life contours plotted in term of log of life for 5083-87 aluminum alloy with SAETRN loading by using strain-life method.

**Material Optimization**

The material optimization was done to determine the suitable material for the suspension arm. The comparison was made in a series of aluminum alloy such as 2014-T6, 3004-H36, 5052-H32, 5083-87, 6061-T6 and 7175-T73. The effect of mean stress correction method such as Goodman mean stress correction and Smith-Watson Topper (SWT) mean stress correction are considered in this study. The implementation of these optimizations is to find out which is the better method to improve the fatigue life of the suspension especially at the critical location. The results of material optimization based on various loading histories are shown in Table 6. 7175-T73 aluminum alloy has the higher life compared to other materials based on SAETRN loading histories at the critical location of node (8408). It is obviously seen that Table 6, Goodman method is more conservative method compared to SWT method for SAETRN and SAESUS loading condition while SWT method is more conservative in SAEBKT loading histories. Referring to Table 6, less life is predicted using the variable amplitude loading of SAEBKT compared to SAETRN and SAESUS time histories. Thus it can be said that the minimum predicted fatigue life at the critical location at node (8408) of the suspension is strongly related to variable amplitude loading. The acquired results show that, 7175-T6 gives higher fatigue life for the suspension arm.

Table 6: Comparison between the different materials for various loading time histories using stress-life and strain-life method.

| Loading Cond. / Materials (Al Alloys) | Prediction fatigue life at critical location (cycles) | | | | | |
|---|---|---|---|---|---|---|
| | SAETRN | | SAESUS | | SAEBKT | |
| | Goodman | SWT | Goodman | SWT | Goodman | SWT |
| 2014-T6 | 1047 | 537 | 5370 | 2238 | 389 | 316 |
| 3004-H36 | 199 | 472 | 482 | 873 | 120 | 94 |
| 5052-H36 | ** | 128 | ** | 794 | ** | 28 |
| 5083-87 | 251 | 323 | 588 | 1514 | 194 | 120 |
| 6061-T6 | ** | 457 | 9.55 | 2089 | 7.74 | 141 |
| 7175-T73 | 8511 | 2630 | 61659 | 11748 | 10471 | 2041 |

** Broken

## CONCLUSION

From the analysis conducted, several conclusions can be drawn as follows.

(i) Prediction of the fatigue life is focused on critical location of node 8408.

(ii) Goodman method is conservative method when subjected to SAETRN and SAESUS loading histories while SWT method is applicable in SAEBKT loading histories.

(iii) Stress-life method is capable to give higher fatigue life when subjected to bracket mean loading (SAEBKT) while strain-life method is capable to give higher fatigue life when subjected to positive mean loading (SAETRN) and negative mean loading (SAESUS).

(iv) 7175-T73 is suitable material compared to others material in the optimization.

## ACKNOWLEDGEMENT

The authors would like to thank Faculty of Mechanical Engineering, Universiti Malaysia Pahang for provided laboratory facilities.

## REFERENCES

Coffin, L.F. 1954. A study of the effects of cyclic thermal stresses on a ductile metal. Transactions of ASTM, 76: 931-950.

Conle, F.A. and Mousseau, C.W. 1991. Using vehicle dynamic simulation and finite element result to generate fatigue life contours for chassis component. International Journal of Fatigue, 13 (3): 195 - 205.

Kim, H.S, Yim, H.J and Kim, C.M. 2002. Computational durability prediction of body structure in prototype vehicles. International Journal of Automotive Technology, 3(4): 129-136.

Kyrre, S.A., Skallerud, B., Tveiten, W.T. and Holme, B. 2005. Fatigue life prediction of machined components using finite element analysis of surface topography, International Journal of Fatigue, 27: 1590- 1596

Manson, S.S. 1953. Behavior of materials under conditions of thermal stress. Heat Transfer Symposium, pp. 9-75.

Matsuishi, M. and Endo, T. 1968. Fatigue of metals subjected to varying stress. Presented to JSME, Fukuoko, Japan.

Miner, A., 1945. Cumulative damage in fatigue. Journal of Applied Mechanics, 12: 159-164.

Molent, L., McDonald, M., Barter, S. and Jones, J. 2007. Evaluation of spectrum fatigue crack growth using variable amplitude data. International Journal of Fatigue, 30(1): 119-137

Morrow, J. 1968. Fatigue Design Handbook: Advances in Engineering. Warendale, PA: SAE, 21-29.

Nadot, Y. and Denier, V. 2003. Fatigue failure of suspension arm: experimental analysis and multiaxial criterion. International journal of Fatigue, 11(4): 485 – 499.

Palmgren, A., 1924. Durability of ball bearings. ZVDI, 68(14): 339-341.

Rahman, M.M., Ariffin, A.K., Abdullah, S. and Jamaludin, N. 2007. Finite element based durability assessment of a free piston linear engine component. SDHM, 3(1): 1-13.

Rahman, M.M., Kadirgama, K., Noor, M.M., Rejab, M.R.M., Kesulai, S.A. 2009. Fatigue life prediction of lower suspension arm using strain-life approach. European Journal of Scientific Research, 30(3): 437-450.

Smith, K.N., Watson, P. and Topper, T.H. 1970. A stress-strain functions for the fatigue on materials. Journal of Materials. 5(4): 767-78.

Stephens, R.I., Fatemi, A., Stephens, R.R. and Fuchs, H.O. 2000. Metal fatigue in engineering. New York: John Wiley & Sons, Inc.

Svensson, T., Johannessona, P. and Mare´a, J.D. 2005. Fatigue life prediction based on variable amplitude tests—specific applications. International Journal of Fatigue, 27: 966–973.